Three-Dimensional Structure of the Cytoplasmic Face of the G Protein Receptor Rhodopsin†

Philip L. Yeagle,*,‡ James L. Alderfer,§ and Arlene D. Albert*,‡

Department of Biochemistry, School of Medicine and Biomedical Sciences, University at Buffalo, Buffalo, New York 14214, and Department of Biophysics, Roswell Park Cancer Institute, Buffalo, New York 14263

Received April 21, 1997; Revised Manuscript Received June 12, 1997⊗

ABSTRACT: Rhodopsin is a G protein receptor from a many-membered family of membrane receptors. No high-resolution structure exists for any member of this family due to the insolubility of membrane proteins and the difficulty in crystallizing membrane proteins. Two new approaches to the structure of rhodopsin are described that circumvent these limitations: (1) individual solution structures of the four cytoplasmic domains of rhodopsin are fitted with the transmembrane domain; (2) the solution structure of a complex of the four cytoplasmic domains is determined from nuclear magnetic resonance data. The two structures are similar. To test the validity of these structures, specific site-to-site distances measured on intact membrane-bound rhodopsin are compared to the same distances on the structures reported here. Excellent agreement is obtained. Furthermore, the agreement is obtained with distances measured on the activated form of the receptor and not with distances on the dark-adapted form of rhodopsin. This approach may prove to have general applicability for the determination of the structure for membrane proteins.

Rhodopsin is a member of the family of G-protein receptors that promote signal transduction in a wide variety of cellular systems (Freissmuth et al., 1989). The signal is transduced by receptor activation of heterotrimeric G proteins, which in turn regulate target enzymes, ion channels, and intracellular signaling pathways. A question critical to an understanding of the mechanism of activation of these signal transduction systems is the structure of the receptor. However, no high-resolution structure of any G protein receptor is known. Normal crystallographic approaches to the study of the structure of rhodopsin have not yet been successful, and because the protein is too large and not soluble, multidimensional nuclear magnetic resonance (NMR)[1] techniques cannot be used on intact rhodopsin.

Therefore, an alternative means is required to obtain the critical three-dimensional structural information necessary to understand the function of this receptor. The body of available evidence suggests that ordered structures of protein fragments in solution reflect the structures of the parent proteins, particularly when the fragments contain β-turns (see below). Recently, we reported that the four cytoplasmic domains of rhodopsin, three cytoplasmic loops and the carboxyl-terminal domain, have defined structure in solution (Yeagle et al. 1995a,b, 1996, 1997). The third cytoplasmic loop has an α-helix on one side of the loop as an extension of transmembrane helix 5, as is also observed for the third cytoplasmic loop of the PTH receptor (Mierke et al., 1996). Each of the other two cytoplasmic loops forms loops in solution independent of the rest of the protein and stabilized by β-turns. The carboxyl terminus contains an extension of helix 7, forms the fourth cytoplasmic loop with the palmitoylation sites at the bottom of the loop next to the membrane surface, and at the carboxyl terminus forms a short antiparallel β-sheet with a β-turn containing the rhodopsin kinase (Palczewski et al., 1988) and protein kinase C sites (Greene et al., 1997). These observations open an alternate approach to the structure of rhodopsin.

Two methods are used which produce similar structures. (1) The experimentally determined structures of the four cytoplasmic domains of rhodopsin are fitted to the structure of the transmembrane domain to build the cytoplasmic face of this receptor. (2) Three of these domains (second and third cytoplasmic loops and the carboxyl-terminal domain) have biological activity in solution and are synergistic in their ability to inhibit the activation of the G protein by light-activated rhodopsin (Konig et al., 1989). The latter data suggest that three of the domains may form a complex in solution. Circular dichroism data confirm this suggestion. The structure of this complex (with the addition of the first cytoplasmic loop) is determined from multidimensional NMR data. This structure is similar to the structure obtained by the first procedure.

The fidelity with which the structure determined in this report reflects the structure of the native protein is tested by comparing the structure with several point-to-point distances recently measured on intact rhodopsin. Spin labels have been introduced into specific sites on the protein, and the distance between them has been determined (Farrens et al., 1996; Yang et al., 1996b). Excellent agreement is obtained between these distance measurements on the protein and the same distances in the structure reported here. Furthermore, the agreement is with the structure of the R*, or activated, form of the receptor.

† This work was supported by National Institutes of Health Grant EY03328 and in part by Grant CA16056.

* Corresponding author.

‡ Department of Biochemistry, School of Medicine and Biomedical Sciences, University at Buffalo.

§ Department of Biophysics, Roswell Park Cancer Institute.

⊗ Abstract published in *Advance ACS Abstracts,* July 15, 1997.

[1] Abbreviations: CD, circular dichroism; NMR, nuclear magnetic resonance; R, dark adapted state of rhodopsin; R*, activated state of rhodopsin; rhoI, the first cytoplasmic loop of rhodopsin; rhoII, the second cytoplasmic loop of rhodopsin; rhoIII, the third cytoplasmic loop of rhodopsin; rhoIV, the carboxyl-terminal domain of rhodopsin.

S0006-2960(97)00908-2 CCC: $14.00

MATERIALS AND METHODS

Peptides corresponding to each of the four cytoplasmic domains of rhodopsin were synthesized by solid-phase peptide methods at the Biopolymer Facility, Roswell Park Cancer Institute, using FMOC chemistry: for the first cytoplasmic loop, a 17mer labeled rhoI (residues 60−76), for the second cytoplasmic loop, a 16mer labeled rhoII (residues 139−154), for the third cytoplasmic loop, a 26mer labeled rhoIII (residues 231−256), and for the carboxyl-terminal domain, a 43mer labeled rhoIV (residues 306−348). They were purified by HPLC, the amino acid composition was analyzed, and the primary sequence was determined.

Circular Dichroism Spectroscopy. Circular dichroism (CD) spectra were obtained on a JASCO J-600 spectropolarimeter at room temperature, with a path length of 0.1 cm, a bandwidth of 1.0 nm, a time constant of 2.0 s, and a wavelength range of 260−185 nm, using quartz cuvettes. The spectrum for the buffer was subtracted from all the other spectra.

NMR Spectroscopy. All NMR spectra were accumulated in 1.0 mM phosphate buffer at pH 5.9 on a Bruker AMX-600 spectrometer at 10 °C at a peptide concentration of 1.3 mM. Standard pulse sequences and phase cycling were employed to record in H_2O (10% D_2O), double-quantum-filtered (DQF) COSY and NOESY (400 ms mixing time) (Kumar et al., 1980). Previous work on the individual peptides showed the largest amount of information at this mixing time. Comparison of the data obtained in this study to the previous data from the individual peptides revealed no evidence of spin diffusion. All spectra were accumulated in a phase-sensitive manner using time-proportional phase incrementation for quadrature detection in F_1. The sequence-specific assignment of the ^{1}H NMR spectrum of the complex was carried out as described previously (Yeagle et al. 1995a,b, 1996). Differences in the CαH chemical shifts from the individual peptides and from the peptides in the complex were minor (most in the range of ±0.02 ppm). The few resonances with greater changes are discussed below. Assigned NOE cross peaks were segmented using a statistical segmentation function and characterized as strong, medium, and weak corresponding to upper bounds distance range constraints of 2.7, 3.7, and 5.0 Å, respectively. Lower bounds between nonbonded atoms were set to the sum of their van der Waals radii (approximately 1.8 Å). Pseudoatom corrections were added to interproton distance restraints where necessary (Wüthrich et al., 1983).

Internuclear distances on the structures were measured using MacImdad, and Sculpt calculations were performed on a Power Macintosh 8500. All other calculations were performed on an SGI 4D/440.

RESULTS AND DISCUSSION

Fitting of Cytoplasmic Domains to the Transmembrane Domain of Rhodopsin. First to be addressed is the question: do the peptides representing the cytoplasmic domains of rhodopsin reflect the structure of the parent protein? Previous experiments have demonstrated that peptides representing each of the cytoplasmic domains of rhodopsin exhibit ordered structure in solution, and three of the four contain β-turns (see above). These peptides also exhibit thermal transitions (differential scanning calorimetry) consistent with a stable solution structure (Albert and Epand, unpublished data). Data from several laboratories show that the carboxyl-terminal domain of rhodopsin and two of the cytoplasmic loops inhibit transducin activation (GTP−GDP exchange), resultant downstream phosphodiesterase activity, and rhodopsin kinase activity (Takemoto et al., 1985, 1986; Konig et al., 1989; Yeagle et al. 1995a,b), while facilitating the activation of the α subunit of transducin (Phillips & Cerione, 1994). Therefore, these peptides exhibit stable structure in solution and biological activity. The simplest explanation of these data is that the peptide in solution assumes a conformation similar to that exhibited in the native protein and thus can bind to the G protein and interfere with rhodopsin binding. This explanation is supported by the data on binding of peptide antigens to antibodies that retain the solution structure on binding to the antibody, especially when the peptide contains a β-turn (Chandrasekhar et al., 1991; Blumenstein et al., 1992; Ghiara et al., 1994; Campbell et al., 1995).

The issue of independent stabilization of protein domains has been extensively investigated. The conclusion is that many proteins, including membrane proteins, can be divided into domains which form a three-dimensional structure characteristic of the native protein, independently of interactions with other domains of the same protein (Albert & Litman, 1978; Schulte & Marchesi, 1979; Esmann et al., 1994). Structural determinations have shown that protein fragments, when they exhibit structure in solution, reflect the structure observed in the intact protein (Blanco & Serrano, 1994; Goudreau et al., 1994). This is particularly true when the peptides contain a β-turn (Chandrasekhar et al., 1991; Blumenstein et al., 1992; Adler et al., 1995), as is the case with three of the four cytoplasmic domains of rhodopsin. This stabilization of structure can be understood in the context of the report that the β-turn is stabilized primarily by short-range interactions (Yang et al., 1996a). These data predict that the cytoplasmic domains of rhodopsin are expected to show structure characteristic of the native protein since they exhibit stable structures containing β-turns in solution and three of the four are biologically active.

A structure can be built from these cytoplasmic domains of rhodopsin. Low-resolution information on the structure of the transmembrane domain of rhodopsin has been reported (Schertler et al., 1993). A model of that domain is constructed, using the helix assignment and rotational orientation (of the helices) proposed by Baldwin (1993). A structure of the cytoplasmic face of rhodopsin is obtained by fitting the experimentally determined structures of the four cytoplasmic domains to the transmembrane domain. In several cases, such as the carboxyl-terminal domain (Yeagle et al., 1996) and the third cytoplasmic loop (Yeagle et al., 1997), fitting is achieved by overlap of the helix in the structure of the cytoplasmic domain with the appropriate helix of the transmembrane domain. In the case of the second cytoplasmic loop, while the helices of the loop are more open than α-helices, they nevertheless represent a logical unwinding of the transmembrane helix and can be readily fitted with the appropriate transmembrane helix. The ends of the first cytoplasmic loop are not well ordered in the original structure determination, but it is possible to position the loop over the ends of helices 1 and 2 and thus locate it correctly relative to the other cytoplasmic domains. This procedure organizes the cytoplasmic domains relative to each other. The energy of the structure, without the

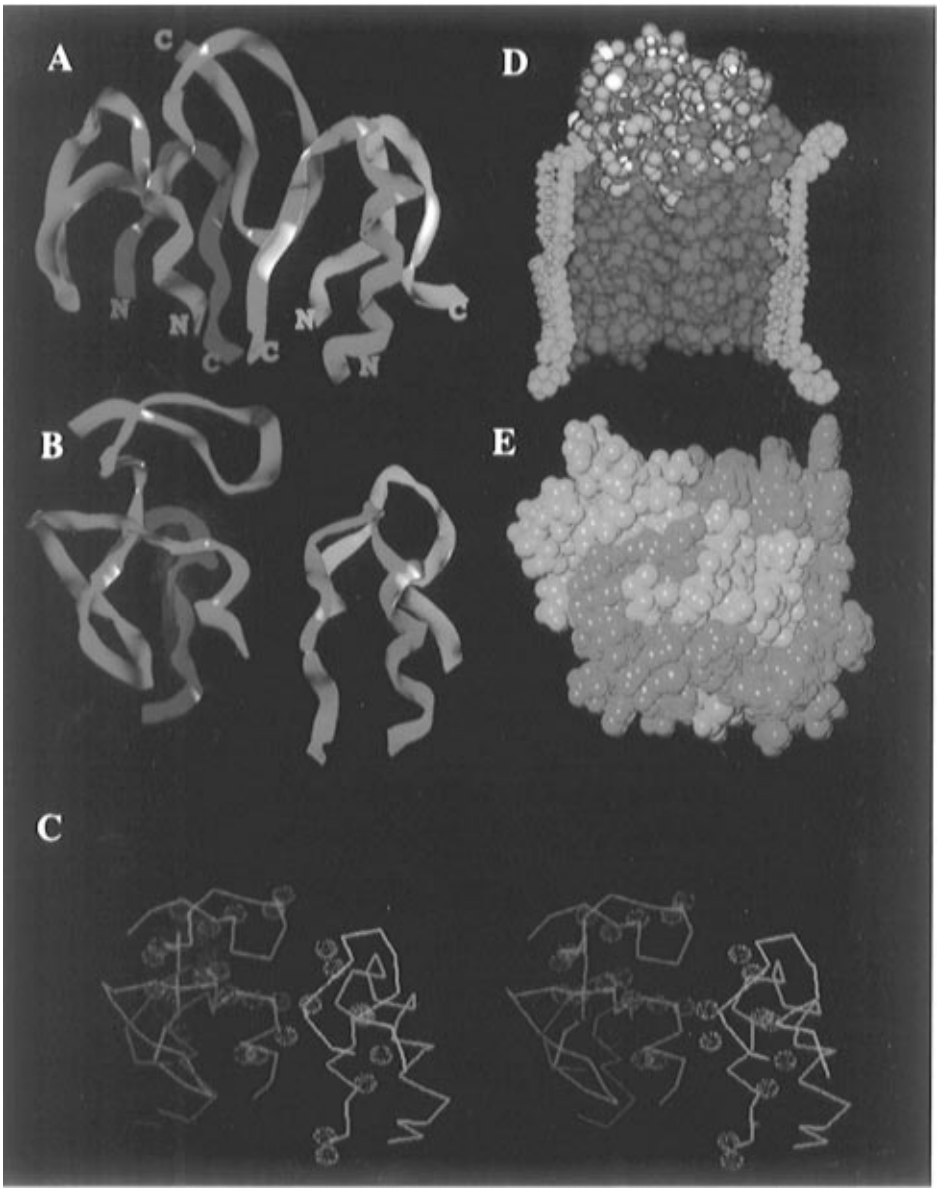

FIGURE 1: Structure of the cytoplasmic face of rhodopsin. (A) The structures of the four cytoplasmic domains (first, second, and third cytoplasmic loops and the carboxyl-terminal domain) were determined as described previously (Yeagle et al., 1995a,b, 1996, 1997). A ribbon structure of the cytoplasmic face, with the carboxyl-terminal domain (magenta) and the third cytoplasmic loop (green), left to right and in front of the figure, and the first cytoplasmic loop (blue) and the second cytoplasmic loop (cyan), left to right in the back of the figure, is shown. (B) Average structure of the 16 structures in Figure 3, with the same color coding as in panel A. (C) Stereoview of the structure in (B) showing atoms with significant changes in ^{1}H chemical shifts (see text) with stippled spheres. (D) Schematic representation of the structure of rhodopsin. The multicolored portion is the structure of the cytoplasmic face of rhodopsin determined in this study. A model of the seven transmembrane helices of rhodopsin was built to match published electron density maps and helix assignment (Baldwin, 1993; Schertler et al., 1993; Unger & Schertler, 1995) and energy minimized in Sculpt. These helices are represented in red. In cyan, four phospholipid molecules are represented in the approximate position of the phospholipid bilayer. (E) View showing the surfaces on rhodopsin (in green) putatively in contact with transducin when the G protein is bound to the activated receptor (see text for details). The blue area in the upper left is from loop 1 which is not biologically active. The blue area in the middle is from the carboxyl terminus (including the true C-terminus of the protein) of rhodopsin, the part of the carboxyl-terminal domain which has not been implicated in contact with the G protein. The orientation is the same as in panel B.

transmembrane helices, was then minimized in the force field in Sculpt (Interactive Simulations, San Diego, CA). For most of the minimization, the peptide ends were constrained to their fitted positions. During the last cycles of minimization, the conformations of the peptides were not restricted. The resulting structure is shown in Figure 1A.

Structure of a Complex of the Four Cytoplasmic Domains of Rhodopsin. Since activity data suggested that the three biologically active peptides might form a complex which would be useful in structure determinations, CD was used to explore whether such a complex actually formed. CD spectra were obtained separately of each biologically active peptide in solution and of a solution containing all the biologically active peptides. The CD spectrum for the buffer was subtracted from all the other spectra. Figure 2 shows two spectra. One is the sum of the CD spectra from each of the peptides by themselves, and the other is the spectrum of the peptides in solution together. The difference between the spectrum of the sum and the spectrum of the cosolubilized peptides suggests that the three peptides interact in solution. The agreement between the two spectra in the range from 210 to 260 nm suggests that the secondary structure (α-helix,

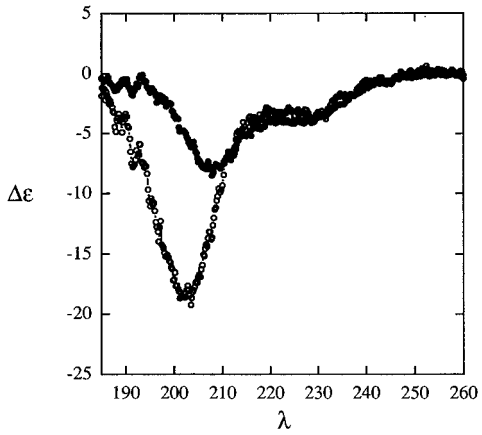

FIGURE 2: CD spectra of the peptides representing the four cytoplasmic domains of rhodopsin. CD data were obtained on a JASCO J-600 spectropolarimeter at room temperature, with a path length of 0.1 cm, a bandwidth of 1.0 nm, a time constant of 2.0 s, and a wavelength range of 260−185 nm, and using quartz cuvettes. The peptides were examined at 55 μM in 1 mM phosphate buffer, pH 5.9, at 23 °C. (○) Sum of CD spectra of individual peptides in solution. (●) CD spectra of an equimolar solution of the three biologically active peptides.

β-turn, and β-sheet in this case) does not change significantly when the three peptides interact. The difference between the two spectra at about 200 nm suggests that separately the three peptides exhibit some disordered structure that is ordered upon interacting with each other (Venyaminov & Yang, 1996). These data indicate that a complex is formed and are in agreement with what is observed (below) from the structure determination.

The structure of this complex, with the addition of the first cytoplasmic loop, was determined by multidimensional NMR. A total of 1119 constraints were used: 653 intraresidue, 285 sequential, 174 long range, and 7 intermolecular. The seven intermolecular constraints were between the following residues, using the numbering of the entire rhodopsin sequence: Arg252 (rhoIII) ↔ Asn310 (rhoIV); Arg147 (rhoII) ↔ Lys245 (rhoIII); Tyr60 (rhoI) ↔ Met309 (rhoIV); Met308 (rhoIV) ↔ Tyr74 (rhoI); His65 (rhoI) ↔ Phe313 (rhoIV); Lys66 (rhoI) ↔ Cys322 (rhoIV); Phe146 (rhoII) ↔ Thr342 (rhoIV). The limited number of intermolecular constraints was due to the density of peaks in the NOESY data. Only peaks in relatively less dense regions of the NOESY map, for which an unambiguous assignment of the peaks was determined as intermolecular, were used. Four molecules, representing the four cytoplasmic domains solved previously, were loaded into SYBYL. Starting with the above described fitted structure, simulated annealing was performed using the experimental NOE constraints and 16 structures were generated. Energy refinement calculations (restrained minimizations/dynamics) were carried out on each of the structures using the SYBYL program implementing the Kollman all-atom force field. Figure 3 shows the overlay of the 16 structures calculated. Figure 1B shows the average structure. The structure in Figure 1B is similar to the structure in Figure 1A. The only major difference is the greater exposure of the β-sheet of the carboxyl-terminal domain in Figure 1B which contains the rhodopsin kinase sites.

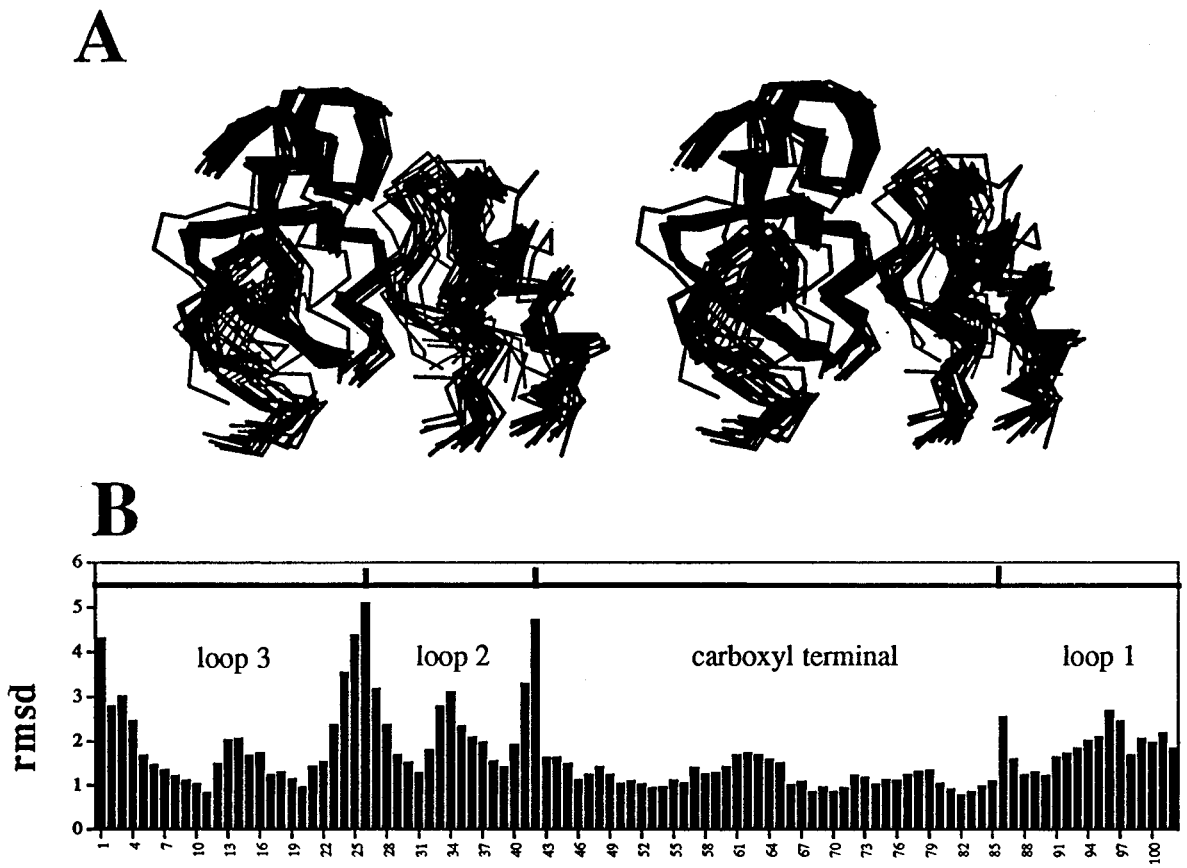

FIGURE 3: (A) Overlay of 16 structures of a complex of the four cytoplasmic domains, obtained from simulated annealing in SYBYL 6.2 (Tripos Software Inc., St. Louis, MO) using the constraints from the NMR NOESY data, with heating to 1000 K for 500 fs, followed by cooling to 300 K for 500 fs. The resulting structures were subjected to energy minimization in SYBYL. (B) Statistics graphed by amino acid position for all of the backbone atoms in the structure. Statistics on structures were obtained from X-PLOR.

Table 1: Distances between Side Chains of Specific Amino Acid Residues in Rhodopsin, Measured on the Structure in This Paper, and the Same Distances Reported Recently on Intact Rhodopsin (Farrens et al., 1996; Yang et al., 1996b)[a]

	this structure[b] (Å)	R* (Å)	R (Å)
Val139 → Lys248	25 ± 2	23−25	12−14
Val139 → Glu249	20 ± 2	15−20	15−20
Val139 → Val250	13 ± 2	12−14	15−20
Val139 → Thr251	19 ± 3	23−25	12−14
Val139 → Arg252	11 ± 3	23−25	15−20
His65 → Met316	12 ± 2	12−15	7−10

[a] R* is the activated form of rhodopsin, and R is the dark-adapted state of rhodopsin. [b] The standard deviation presented is that derived from the distances measured in the ensemble of 16 structures from Figure 3. The measurements are made from the most distal atoms on the side chain to approximate the position of the spin label.

Changes in the chemical shifts as large as 0.09 ppm for a few hydrogens between the individual peptides and the complex were observed. Those hydrogens with changes in chemical shifts of 0.03 ppm or greater are mapped on the structure in Figure 1C. Those hydrogens are largely clustered at the interface between subunits as expected.

Comparison of the Structure for the Cytoplasmic Face to Intact Rhodopsin. The structure reported here can be validated by comparison to the whole protein. Distance measurements have been made between specific sites on intact, activated rhodopsin which are in good agreement with the structure reported here. The laboratories of Khorana and Hubbell have made site-directed mutations to introduce cysteines at specific positions in intact rhodopsin (Altenbach et al., 1996; Farrens et al., 1996). These sites were specifically spin labeled. Using the dipolar interactions between the spin labels, distances between specific sites on rhodopsin were measured in both the R and R* state. Table 1 compares these distances from the native protein with the same distances measured on the structure reported here. The structure reported here is in excellent agreement with the structure of the activated receptor. This suggestion is in agreement with the observation of biological function associated with three of the four domains. The structures in Figure 3 were obtained without the constraints from the spin label data. When these constraints were added to the simulated annealing, little change was observed in the structure since the structures in Figure 3 already satisfied five of these additional constraints.

The structure of the cytoplasmic face of rhodopsin exhibits several interesting features which are in agreement with suggestions from previously published data. This surface of rhodopsin has some β structure, both in turns in the loops and in a small antiparallel sheet in the carboxyl-terminal domain. These structural features are in good agreement with conclusions from FTIR studies on native rhodopsin (Pistorius & deGrip, 1994). Transmembrane helix 5 extends beyond the hydrophobic region of this membrane protein into the third cytoplasmic loop, consistent with those FTIR data and recent spin label experiments (Altenbach et al., 1996). The cross-sectional area of the cytoplasmic face of rhodopsin determined in this work has dimensions of about 33 by 36 Å, in good agreement with previous low-resolution measurements which modeled rhodopsin with a cylinder of diameter approximately 36 Å (Sardet et al., 1976; Osborne et al., 1978). Previous work on boundary lipids with spin-labeled lipids predicts a protein circumference consistent with that in Figure 1 (Watts et al., 1979). The palmitoylation sites on rhodopsin (Cys322 and Cys323) are located at the putative membrane surface on the perimeter of the protein in this structure, where they can be readily acylated (Morrison et al., 1991). In this structure, the fourth cytoplasmic loop forms without being acylated. That may explain why palmitoylation was found to be nonessential to the activation of rhodopsin (Karnik et al., 1993). Finally, the CD data reported here predict that the structure of the complex is more ordered than the structures of the individual peptides. Comparison of the structure in Figure 3 with the previously published structures (Yeagle et al., 1997) shows that the ends of the loops are more ordered in the complex than individually. (Most of the variation in position in the figure is due to the low number of intermolecular NOEs obtained. Overlay of the 16 structures of any one of the individual loops shows much better agreement.) Together, the body of data available on native rhodopsin is in excellent agreement with the structure of the cytoplasmic surface presented here.

Structural Features. Analysis of the structure reveals some indication for the molecular basis for the apparent stability of the complex. Three salt bridges are observed in the structure. Two involve lysines and glutamates: one between rhoII (Glu150) and rhoIII (Lys245) and the other between rhoIII (Glu249) and rhoIV (Lys311). The third salt bridge involves lysine (66) and aspartate (330), between rhoI and rhoIV. Some of the larger chemical shift changes mentioned previously map to these salt bridges.

Three helices can be seen in the structures in Figure 1: one on the carboxyl-terminal domain, one part of the third cytoplasmic loop [a similar helix is seen in a peptide representing the third cytoplasmic loop of the PTH/PTHrP receptor (Mierke et al. 1996)], and one small helix at the C-terminal end of the second cytoplasmic loop. These results suggest that at least three of the transmembrane helices of rhodopsin extend beyond the hydrophobic transmembrane domain. Furthermore, these helices clearly mark the connection with the transmembrane domain, and the location of these helices agrees well with the low-resolution structure of the transmembrane domain reported previously (Schertler et al., 1993). One difference is in the position of the cytoplasmic end of helix 3, which in the structure reported here is further from helix 6 than in the Schertler structure. This is in remarkable agreement with the distance measurements from the specific spin-labeling results. The latter data predict that helix 3 and helix 6 should be closer together in the dark-adapted state, as in the Schertler structure, whereas in the activated state helix 3 and helix 6 should be further apart, as in the structure reported here.

The relationship between the structure of the cytoplasmic face of rhodopsin determined here and the remainder of the protein is schematically represented in Figure 1D. The transmembrane helical bundle is represented in red, modeled on the structure of Schertler et al. (1993). For reference purposes, four phospholipid molecules are also included, at the approximate position of the phospholipid bilayer.

Previous studies have identified sequences within the cytoplasmic face of rhodopsin which are inhibitory to activation of transducin and have been suggested to be at the rhodopsin−transducin interface. Figure 1E shows these regions in green. While much of the receptor face is apparently involved in the interface, the middle region,

containing a significant part of the carboxyl-terminal domain including the true C-terminus of the protein, appears uninvolved. This observation is consistent with available data. The β-adrenergic receptor has a much larger carboxyl-terminal domain than rhodopsin, yet both can interact with the same G protein (Cerione et al., 1985). When rhodopsin and transducin bind, the carboxyl-terminal domain must not fill all the available space between receptor and G protein. That space would likely be more effectively filled when the β-adrenergic receptor is involved. Thus in rhodopsin, not all the carboxyl-terminal domain would be expected to be in contact with transducin.

The agreement with the structures in Figure 1 and the activated form of the receptor, R*, suggests an interesting hypothesis on the activation of rhodopsin. Since it forms readily, this structure could be considered a partially "relaxed" structure. The 11-*cis*-retinal may function like an antagonist, holding rhodopsin in an unactivated state, until the absorption of a photon of light (Rao & Oprian, 1996). As has been well studied, light stimulates an excited state isomerization to *all-trans*- retinal, which allows the transient formation of metarhodopsin II, the active form of the receptor. In terms of structure this may mean a relaxation of the cytoplasmic face of rhodopsin to the structure in Figure 1 as 11-*cis*-retinal is rendered impotent as an antagonist by light. Since helix 3 and helix 6 are further apart in R* than in R, the activation of the receptor likely involves an expansion of the volume of the receptor in the plane of the membrane as predicted previously (Lamola et al., 1974; Mitchell et al., 1992). This conformational change in rhodopsin may be the means by which the receptor communicates with the G protein.

Summary. This structure of the cytoplasmic face of rhodopsin represents a significant advance for the understanding of visual transduction, as well as for the structure of other related receptors and mammalian membrane proteins in general. It provides the first detailed structural information on any G protein receptor and a potential alternate paradigm for securing three-dimensional structural information on other membrane receptors and more generally on integral membrane proteins. This research will also open an entirely new field of drug discovery.

ACKNOWLEDGMENT

We thank Drs. V. Cody and R. Wollman for assistance in calculations.

REFERENCES

Adler, M., Sato, M. H., Nitecki, D. E., Lin, J.-H., Light, D. R., & Morser, J. (1995) *J. Biol. Chem. 270*, 23366−23372.

Albert, A. D., & Litman, B. J. (1978) *Biochemistry 17*, 3893−3900.

Altenbach, C., Yang, K., Farrens, D. L., Farahbakhsh, Z. T., Khorana, H. G., & Hubbell, W. L. (1996) *Biochemistry 35*, 12470−12478.

Baldwin, J. M. (1993) *EMBO J. 12*, 1693−1703.

Blanco, F. J., & Serrano, L. (1994) *Eur. J. Biochem. 230*, 634−649.

Blumenstein, M., Matsueda, G. R., Timmons, S., & Hawiger, J. (1992) *Biochemistry 31*, 10692−10698.

Campbell, A. P., McInnes, C., Hodges, R. S., & Sykes, B. D. (1995) *Biochemistry 34*, 16255−16268.

Cerione, R. A., Staniszewski, C., Benovic, J. L., Lefkowitz, R. J., Caron, M. G., Gierschik, P., Somers, R., Spiegel, A. M., Codina, J., & Birnbaumer, L. L. (1985) *J. Biol. Chem. 260*, 1493−1500.

Chandrasekhar, K., Profy, A. T., & Dyson, H. J. (1991) *Biochemistry 30*, 9187−9194.

Esmann, M., Karlish, S. J. D., Sottrup-Jensen, L., & Marsh, D. (1994) *Biochemistry 33*, 8044−8050.

Farrens, D. L., Altenbach, C., Yang, K., Hubbell, W. L., & Khorana, H. G. (1996) *Science 274*, 768−770.

Freissmuth, M., Casey, P. J., & Gilman, A. G. (1989) *FASEB J. 3*, 2125−2131.

Ghiara, J. B., Stura, E. A., Stanfield, R. L., Profy, A. T., & Wilson, I. A. (1994) *Science 264*, 82−85.

Goudreau, N., Cornille, F., Duchesne, M., Parker, F., Tocqué, B., Garbay, C., & Roques, B. P. (1994) *Nat. Struct. Biol. 1*, 898−907.

Greene, N. M., Williams, D. S., & Newton, A. C. (1997) *J. Biol. Chem. 272*, 10341−10344.

Karnik, S. S., Ridge, K. D., Bhattacharya, S., & Khorana, H. G. (1993) *Proc. Natl. Acad. Sci. U.S.A. 90*, 40−44.

Konig, B., Arendt, A., McDowell, J. H., Kahlert, M., Hargrave, P. A., & Hofmann, K. P. (1989) *Proc. Natl. Acad. Sci. U.S.A. 86*, 6878−6882.

Kumar, A., Ernst, R. R., & Wuthrich, K. (1980) *Biochem. Biophys. Res. Commun. 95*, 1−6.

Lamola, A. A., Yamane, T., & Zipp, A. (1974) *Biochemistry 13*, 738−745.

Mierke, D. F., Royo, M., Pellegrini, M., Sun, H., & Chorev, M. (1996) *J. Am. Chem. Soc. 118*, 8998−9004.

Mitchell, D. C., Straume, M., & Litman, B. J. (1992) *Biochemistry 31*, 662−670.

Morrison, D. F., O'Brien, P. J., & Pepperberg, D. R. (1991) *J. Biol. Chem. 266*, 20118−20123.

Osborne, H. B., Sardet, C., Michel-Villaz, M., & Charbre, M. (1978) *J. Mol. Biol. 123*, 177−206.

Palczewski, K., McDowell, J. H., & Hargrave, P. A. (1988) *Biochemistry 27*, 2306−2313.

Phillips, W. J., & Cerione, R. A. (1994) *Biochem. J. 299* (Part 2), 351−357.

Pistorius, A. M., & deGrip, W. J. (1994) *Biochem. Biophys. Res. Commun. 198*, 1040−1045.

Rao, V. R., & Oprian, D. D. (1996) *Annu. Rev. Biophys. Biomol. Struct. 25*, 287−314.

Sardet, C., Tardieu, A., & Luzzati, V. (1976) *J. Mol. Biol. 105*, 383−407.

Schertler, G. R. X., Villa, C., & Henderson, R. (1993) *Nature 362*, 770−772.

Schulte, T. H., & Marchesi, V. T. (1979) *Biochemistry 18*, 275−280.

Takemoto, D. J., Takemoto, L. J., Hansen, J., & Morrison, D. (1985) *Biochem. J. 232*, 669−672.

Takemoto, D. J., Morrison, D., Davis, L. C., & Takemoto, L. J. (1986) *Biochem. J. 235*, 309−312.

Unger, V. M., & Schertler, G. F. X. (1995) *Biophys. J. 68*, 1776−1786.

Venyaminov, S. Y., & Yang, J. T. (1996) in *Circular Dichroism and the Conformational Analysis of Biomolecules* (Fasman, G. D., Ed.) pp 69−108, Plenum Press, New York.

Watts, A., Volovski, I. D., & Marsh, D. (1979) *Biochemistry 18*, 5006−5013.

Wüthrich, K., Billeter, M., & Braun, W. J. (1983) *J. Mol. Biol. 169*, 949−961.

Yang, A.-S., Hitz, B., & Honig, B. (1996a) *J. Mol. Biol. 259*, 873−882.

Yang, K., Farrens, D. L., Altenbach, C., Farahbakhsh, Z. T., Hubbell, W. L., & Khorana, H. G. (1996b) *Biochemistry 35*, 14040−14046.

Yeagle, P. L., Alderfer, J. L., & Albert, A. D. (1995a) *Nat. Struct. Biol. 2*, 832−834.

Yeagle, P. L., Alderfer, J. L., & Albert, A. D. (1995b) *Biochemistry 34*, 14621−14625.

Yeagle, P. L., Alderfer, J. L., & Albert, A. D. (1996) *Mol. Vision 2*, http://www.emory.edu/molvis/v2/yeagle.

Yeagle, P. L., Alderfer, J. L., & Albert, A. D. (1997) *Biochemistry 36*, 3864−3869.

BI970908A